OPEN ACCESS
Journal of Innovative Optical Health Sciences
Vol. 14, No. 3 (2021) 2150014 (15 pages)

DOI: 10.1142/S1793545821500140

World Scientific
www.worldscientific.com



# Availability and safety assessment of infrared neural stimulation at high repetition rate through an implantable optrode

Yaqin Wan*, Meiqun Wang†,‡, Shaorong Zhang†,‡ and Bingbin Xie†,‡,§

*Out-Patient Department of the Second Affiliated Hospital of Nanchang University
1 Minde Road, Nanchang 330006, P. R. China

†Department of Otolaryngology Head and Neck Surgery
The Second Affiliated Hospital of Nanchang University
1 Minde Road, Nanchang 330006, P. R. China

‡Jiangxi Biomedical Engineering Research Center for Auditory Research
1 Minde Road, Nanchang 330006, P. R. China
§xiebb2013@163.com

Received 27 March 2021
Accepted 5 April 2021
Published 17 May 2021

An implantable optrode with micro-thermal detectors was designed to investigate the availability and safety of INS using high repetition rates. Optical auditory brainstem responses (oABRs) were recorded in normal-hearing guinea pigs, and the energy thresholds, pulse durations, and amplitudes evoked by the varied stimulus repetitions were analyzed. Stable oABRs could be evoked through INS even as the repetition rate of stimulation reached 19 kHz. The energy threshold of oABRs was elevated, the amplitudes decreased as pulse durations increased and repetition rates were higher, and the latencies were delayed as the pulse durations increased. The temperature variation curves on the site of stimulation significantly increased as the pulse duration increased to 400 $\mu$s. INS elevated the temperature around the stimulus site area via thermal accumulation during radiation, especially when higher repetition stimuli were used. Our results demonstrate that high repetition infrared stimulations can safely evoke stable and available oABRs in normal-hearing guinea pigs.

*Keywords*: Infrared neural stimulation; implantable optrode; cochlear implant; spiral ganglion neuron; optical stimulation.

§Corresponding author.

## 1. Introduction

Hearing loss is the most common form of sensory disorder in humans, affecting people of any age and manifesting in various forms that range from mild to complete deafness. Some estimates suggest that 300 million individuals are affected worldwide.[1] Auditory restoration remains a lofty but achievable goal for patients and scientists. Multiple strategies may ultimately be required to treat hearing loss. Most of these are based on medical devices such as hearing aids and cochlear implants (CIs).[1,2] CIs are considered the most successful neural prostheses, having restored the hearing in nearly 500,000 profoundly deaf adults and children.[3] Contemporary CIs partially restore hearing via direct electrical stimulation of spiral ganglion neurons (SGNs), bypassing the damaged hair cells. However, the major bottleneck limitations to electrical stimulation are the wide-spreading and overlapping currents from each electrode, thereby limiting the spectral coding, ultimately resulting in the limited perception of acoustic signals, such as speech, particularly in noisy environments,[4] and during music appreciation.[5]

Optical neural stimulation has been established as a novel approach with many advantageous features to overcome the limitations of electrical stimulation.[6,7] Optical signals can be confined in space with no stimulation artifacts,[8–10] resulting in greater spatial resolution, and promising artificial sound encoding with increased spectral selectivity. Hence, the technology of optical neural stimulation has been proposed for a new generation of CIs,[9] stimulating smaller SGN populations, and providing a larger number of independent afferent signals, which encode a higher fidelity acoustic information.[11] The users' ability to hear in noisy environments, as well as music appreciation, is likely to improve.

The optical technologies include optogenetics,[12] thermogenetics,[13,14] photoactive tools, nanoparticle-enhanced techniques (such as gold nanoparticles), and direct stimulation of cells — infrared neural stimulation (INS)[15] — using infrared (typically 1400–1600 nm and 1840–2100 nm) or near-infrared (typically 790–850 nm) signals.[16] Optogenetics requires the expression of light-gated ion channels in target neurons by genetic manipulation.[17,18] However, INS does not require any other manipulation. Infrared light is converted into heat directly, no viral sensitization is needed, and no INS-induced photoartefacts can be detected during stimulation.[19] The energy of the INS signal is converted into heat and directly excites the target neurons.[16] Previous studies have demonstrated that infrared-stimulated SGNs could evoke stable auditory brainstem responses (ABRs) and inferior colliculus responses in both normal-hearing and deaf animals.[8,20] Among the pacing factors for the INS technique to translate into CI design are the parameters of infrared stimulation, namely the wavelength, pulse duration, energy density, and stimulus repetition. Most previous experiments *in vivo* and *in vitro* have focused on INS mechanisms, and relevant experimental parameters were mainly selected to make data recording and calculations more convenient. Only a few publications have focused on INS parameters. Izzo *et al.*[21] reported that pulse durations as short as 35 $\mu$s can elicit a compound action potential from the cochlea, while stimulus repetition up to 13 Hz can continually stimulate SGNs. Another study investigating the behavioral and electrophysiological responses evoked by chronic INS of the cochlea selected parameters that better served comparisons with previous data.[22] Most previous studies have selected a low stimulus repetition at 3–10 Hz.[20–22] However, the phase-locking property of the SGN ensures microsecond precision of sound encoding with high fidelity.[23] Thus, the low stimulus repetition at 3–10 Hz leads to loss of sound information, affecting sound perception. The potential risk of INS-induced thermal damage has been previously demonstrated to significantly vary according to tissue type and stimulus repetition.[24] By contrast, shorter pulses generally have a relatively lower margin of energy threshold for damage.[10] When developing an optical CI (oCI) in the future, higher frequency stimulation and optimal pulse duration and energy should be considered when choosing stimulus parameters.

This study aimed to detail different stimulus repetitions and pulse durations in INS, especially focusing on higher stimulation frequencies and longer pulses. We analyzed the availability and safety range of optical parameters to determine the optimal input for INS allowing it to translate into oCI development in the future.

## 2. Materials and Methods

### 2.1. *Animals and hearing assessment*

A total of 10 adult guinea pigs were used (5 male, 5 female; 250–300 g). All animals were assessed by acoustically evoked ABRs (aABRs) to have a normal hearing prior to any other handling. The animals' right and left ears were used for the experimental and control groups, respectively. Ears on both sides underwent the same surgical procedure, a cochleostomy, and the optrode was inserted into the scala tympani of the right ear through the cochleotomy. The left ear was implanted with a shorter fake optrode as a control. In this study, both experimental and control groups consisted of a total of 10 ears. Animal care and use in this study were carried out in accordance with the National Health Commission of the People's Republic of China Guide for the Care and Use of Laboratory Animals and were approved by the Animal Care and Use Committee of the Second Affiliated Hospital of Nanchang University.

The hearing was assessed through aABRs recorded by TDT3 systems (modules RP6, PA5; Tucker-Davis Technologies, Inc., USA). Body temperature was maintained at 38°C by placing the animals on a heating pad (Institute of Biomedical Engineering, China) after fully anesthetizing them by intraperitoneal injection of ketamine (60 mg/kg) and xylazine (4 mg/kg). Three stainless steel electrode needles were placed subcutaneously to obtain aABRs, by subtracting ipsilateral mastoid from vertex potentials measured relative to a ground electrode placed into the nasal apex. The acoustic stimuli were 10-ms tone bursts (including a 1-ms rise time and 1-ms fall time), at frequencies of 8, 16, 24, and 32 kHz. The overall noise during the recordings was reduced by band-pass filtering, with the high-pass and low-pass filter cutoff frequencies set to 300 Hz and 3000 Hz, respectively; the amplifier gain was set to 20 dB.

### 2.2. *Optrode design and fabrication*

An optrode comprising one optical fiber and four micro-probes at the distal end for thermal detection was developed to monitor and simultaneously calculate the temperature variation at the stimulation site (Fig. 1). The optical fiber was a flat polished 200-$\mu$m diameter silica fiber (NA = 0.22)

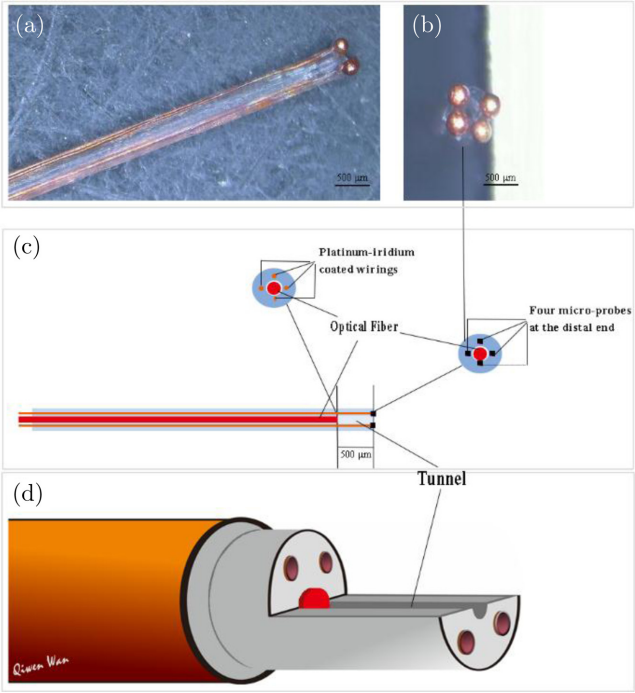


Fig. 1. Images and schematic diagram of the optrode. (a) The distal end of the optrode containing the four micro-probes. (b) The four micro-probes. (c) Diagrams showing the longitudinal and cross-section of the optrode, depicting the optical fiber in the center surrounded with four wirings. The wirings are 500-$\mu$m longer than the center optical fiber, with a tunnel in the center of the optrode allowing the light beam to pass through. The four thermal detector micro-probes were soldered to the end of the wirings to monitor and calculate the temperature variation simultaneously at the location of stimulation. (d) A three-dimensional diagrammatic cross-section of the optrode.

in the center of the optrode, surrounded with platinum–iridium-coated wirings (diameter, 50 $\mu$m; coating, 5 $\mu$m); the wirings were soldered with four micro-probes at the distal end by laser. The optical fiber and the coated wirings were embedded together with biocompatible silica gel MED-4211. A 500-$\mu$m long tunnel (inner diameter, 200 $\mu$m) was inside the distal end of the optical fiber to the micro-probes. The four micro-probes, arrayed around the distal end, were negative temperature coefficient thermistors with a temperature range from −40°C to +125°C. The response time of the micro-probes in liquids was 200 ms, and the accuracy was 0.1°C.

### 2.3. *Animal surgery and preparation for stimulation*

Guinea pigs were anesthetized as above, and medicines were administrated at one-third of the

primary doses throughout the procedures to maintain anesthesia. Signs of increasing arousal were assessed every 30 min by the paw withdrawal reflex. Body temperature was maintained at 38°C via the above-mentioned methods. The animals' heads were stabilized on a head stereotaxic apparatus (SR-6N Stereotaxic Instrument, Narishige Scientific Instrument Lab, Japan), with the right ear up, and in the ventricumbent position. The surgery procedures were described previously.[8] Briefly, a C-shaped retroauricular skin incision was made behind the right ear, and the muscles attached to the bulla and styloid bone were carefully dissected and removed to expose the right bulla. Then, the bulla was opened to access the scala tympani of the cochlea. The optrode was inserted into the scala tympani of the basal turn through the cochleostomy approximately 0.5 mm anterior and inferior to the bony rim of the round window. Using a micromanipulator, the distal end of the optrode was positioned as close as possible to touch the modiolus. The same surgical procedures were implemented on the left ear to implant a shorter fake optrode as a control.

### 2.4. *INS parameters and optical ABR recordings*

Infrared stimuli were received from a benchtop diode infrared laser (SFOLT Co., Ltd., Shanghai, China) with an output wavelength of 1850 nm; pulse durations of 50, 100, 150, 200, 400, 800, and 1000 $\mu$s; and stimulus repetitions of 1–19 kHz. The pulse energy of the laser was controlled directly by varying the diode current. The energy per pulse was measured in air at the distal end of the optical fiber at room temperature, using a J50LP-1A energy sensor (Coherent, Santa Clara, CA). Power ranged between 0 mW and 600 mW (0–60 $\mu$J/pulse and 0–191.08 mJ/cm$^2$ calculated at 100-$\mu$s pulse duration; fiber diameter, 200 $\mu$m). The energy density per pulse $E$ (mJ/cm$^2$) was calculated by $W/\pi r^2$, where $W$ is the energy per pulse ($\mu$J) and $r$ is the sectional area radius of the optical fiber (100 $\mu$m). The optical ABRs (oABRs) were recorded using TDT3 systems. Acoustic stimulus signals were captured from the output port of the PR6 module and converted into a synchronous current pulse to trigger the diode laser generating an infrared pulse to stimulate the

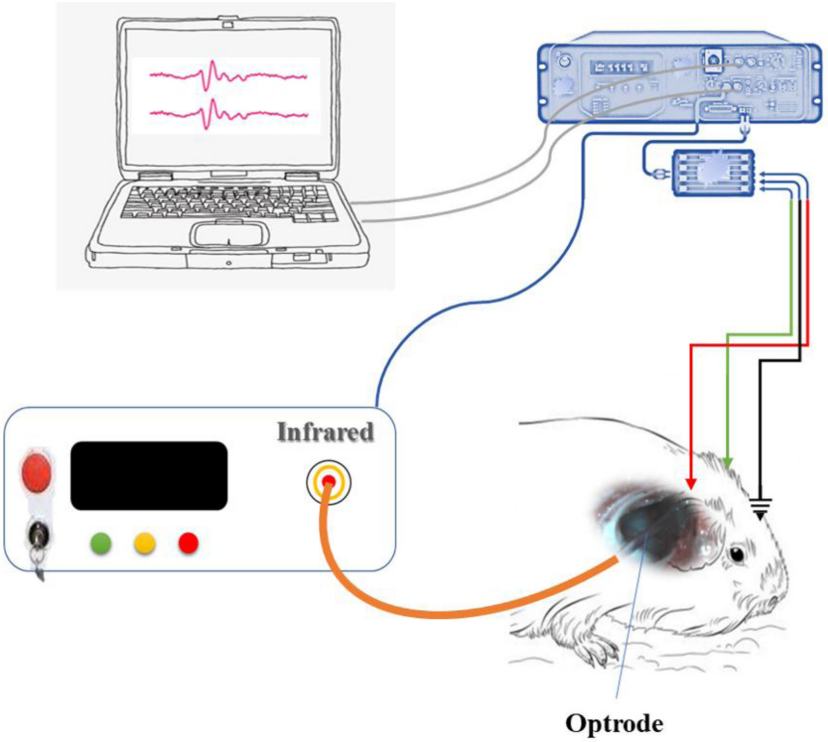


Fig. 2. Schematic diagram of the experiment. Acoustic stimulus signals were captured from the output of the PR6 module (TDT3 systems) and converted into a synchronous current pulse to trigger the diode laser generating an infrared pulse. The infrared pulses were delivered synchronously to the right cochlea of the guinea pig through an optical fiber coupled to an optrode at the distal end. Then, the PR6 module recorded the ABRs. ABR, auditory brainstem response.

cochlea. The infrared pulses and repetition rates were controlled by TDT3 systems. The acquisition parameters were the same as those used during aABR recordings (Fig. 2).

### 2.5. *Statistical analysis*

Means and standard deviations (SDs) were calculated for the energy thresholds and amplitudes of oABRs, as well as INS-induced temperature variations. Analysis of variance (ANOVA) was performed to compare data of energy thresholds and amplitudes of oABRs, and temperature variations recorded from different INS parameters. The hearing levels pre- and post-stimulation between both ears were also analyzed. The Kruskal–Wallis test was used for nonnormally distributed data. If the Kruskal–Wallis test indicated differences among the means, an *a posteriori* test, Tamhane's T2, was used for pairwise comparisons. Results were considered statistically significant if $p < 0.05$. All statistical tests were performed using IBM SPSS 26.0 statistics software.

## 3. Results

The 10 adult guinea pigs used in this study recovered without fever or postoperative incision infection. No animal died during or shortly after INS.

### 3.1. *Longer pulse durations and higher repetition rates increase oABRs thresholds*

The threshold of oABRs was defined as the minimal energy to evoke an oABR wave with the amplitude of wave III higher than 0.5 $\mu$V. The oABRs thresholds were significantly elevated when the pulse duration was longer than 100 $\mu$s (Table 1, Fig. 3). The thresholds were also affected by variations in the stimulus rate. Higher stimulus repetition required higher energy to evoke an oABR wave, especially when the pulse duration was longer than 200 $\mu$s. The thresholds were significantly elevated when the stimulus repetition rate exceeded 500 Hz (Table 2, Fig. 3). There were no significant differences in the thresholds when the pulse duration was up to 100 $\mu$s, even in stimulus repetition rates as high as 1000 Hz.

### 3.2. *oABR latencies across different pulse durations and repetition rates*

To compare the latencies of oABR waves evoked by different pulse durations and repetition rates, an energy intensity of 60 $\mu$J was used to ensure that a recordable wave could be evoked as the stimulus pulse duration and repetition rate varied. Latency was delayed as the pulse duration increased. There were significant changes in latency when the pulse duration increased from 100 $\mu$s to 150 $\mu$s, and from 200 $\mu$s to or over 400 $\mu$s (Fig. 4). The latency was not shortened significantly as stimulus energy intensity increased from 30 $\mu$J to 60 $\mu$J while the pulse duration (50–1000 $\mu$s) and repetition rate (1–1000 Hz) was fixed. When the pulse duration was no longer than 100 $\mu$s, latency was delayed as the stimulus repetition rate increased above 500 Hz. However, latency was delayed stepwise as the repetition rate increased while the pulse duration was longer than 100 $\mu$s.

### 3.3. *oABR amplitude decreases with longer pulse duration and higher repetition rate*

The amplitude of oABRs was calculated from wave III evoked by the energy intensity of 60 $\mu$J in different pulse durations and repetition rates. The amplitudes decreased for pulse durations above

Table 1. Energy thresholds of oABR between different pulse durations (Means ± SD, $n = 10$).

| | 1 Hz | 2 Hz | 10 Hz | 20 Hz | 100 Hz | 200 Hz | 500 Hz | 1000 Hz |
|---|---|---|---|---|---|---|---|---|
| 100 $\mu$s | 7.439 ± 1.096 | 7.389 ± 1.107 | 7.406 ± 1.147 | 7.550 ± 0.882 | 7.894 ± 1.389 | 8.056 ± 1.466 | 11.706 ± 2.359 | 11.426 ± 2.048 |
| 150 $\mu$s | 17.405 ± 2.914 | 16.474 ± 2.334 | 17.460 ± 2.624 | 18.206 ± 3.185 | 19.848 ± 2.210 | 23.835 ± 5.215 | 24.933 ± 4.344 | 25.713 ± 3.011 |
| *F* | 92.2530 | 111.2890 | 110.9560 | 93.5790 | 188.6820 | 76.3510 | 64.4430 | 138.5640 |
| *p* | *0.0000* | *0.0000* | *0.0000* | *0.0000* | *0.0000* | *0.0000* | *0.0000* | *0.0000* |

*Note*: Results were considered statistically significant if $p < 0.05$, $n = 10$.

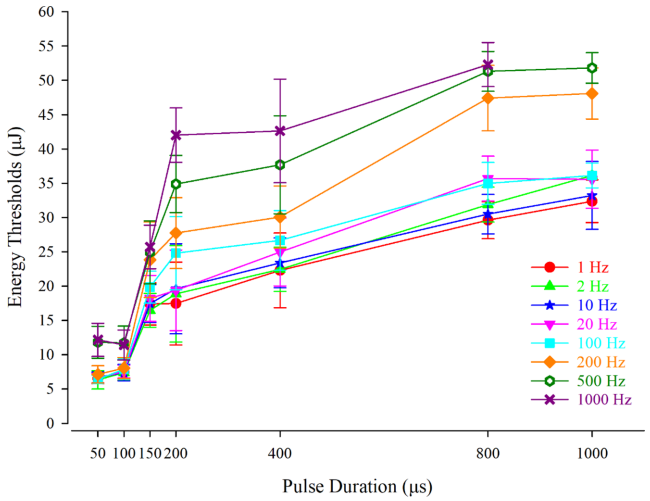


Fig. 3. The energy thresholds of oABRs at different pulse durations and repetition rates. Higher stimulus repetition rates and longer pulse durations require higher energy to evoke an oABR wave. Energy thresholds are significantly elevated ($p < 0.001$, $n = 10$) when the pulse duration is increased from 100 $\mu$s to 150 $\mu$s regardless of the stimulus repetition rate (1–1000 Hz). When the stimulus repetition rate increases to 500 Hz, thresholds become significantly different ($p < 0.001$, $n = 10$), except for a pulse duration of 150 $\mu$s (200 Hz $23.835 \pm 5.215$, 500 Hz $24.933 \pm 4.344$; $F = 0.236$, $p = 0.633$, $n = 10$). oABR, optical auditory brainstem response.

100 $\mu$s (Table 3). There were no significant changes in the amplitude when the pulse duration increased from 50 $\mu$s to 100 $\mu$s, regardless of the level of stimulus repetition rate (Fig. 5). However, the amplitude decreased significantly when the pulse duration increased to 150 $\mu$s (Table 3, Fig. 5). When the amplitudes were compared between different stimulus repetition rates, the results showed that repetition rates up to 500 Hz and pulse durations up to 400 $\mu$s and 800 $\mu$s significantly decreased the amplitude (Table 4, Fig. 5). When the stimulus repetition rate was up to 1000 Hz, the amplitude significantly decreased in most pulse durations except 100 $\mu$s and 50 $\mu$s (Table 4).

### 3.4. *Temperature variations around the stimulus location*

The temperature was monitored and recorded immediately at four different points around the stimulation site at the end of the last pulse, using an energy intensity of 60 $\mu$J. The temperature elevation was calculated as the average of the records from the four points and was associated with both the pulse duration and stimulus repetition rate. The temperature variation increased as the pulse duration became longer, at a constant repetition rate below 1000 Hz. However, there were no differences in temperature elevation when the repetition rate increased from 1 Hz to 2 Hz in any pulse duration (Table 5, Fig. 6). When a pulse duration from 50 $\mu$s to 200 $\mu$s was used, temperature variation became significantly different until the stimulus repetition rate reached 500 Hz. Contrarily, when this rate was $\geq$ 500 Hz, the temperature increased regardless of pulse duration (Table 6, Fig. 6). The temperature elevation was significantly different as the pulse duration became $\geq$ 400 $\mu$s while the stimulus repetition rate reached $\geq$ 10 Hz. The temperature elevation reached 2.67°C when using a 200-$\mu$s pulse duration and 1000 Hz repetition rate, and further increased as the duration became longer.

### 3.5. *oABRs characteristics in high stimulus repetition rates*

We also recorded oABRs using a high stimulus repetition rate ($\geq$ 1000 Hz). The shorter pulse durations of 50 $\mu$s and 100 $\mu$s were used to reach a

Table 2. Energy thresholds of oABR between different stimulus repetitions (Means $\pm$ SD, $n = 10$).

| | 50 $\mu$s | 100 $\mu$s | 150 $\mu$s | 200 $\mu$s | 400 $\mu$s | 800 $\mu$s | 1000 $\mu$s |
|---|---|---|---|---|---|---|---|
| 100 Hz | 6.418 ± 0.542 | 7.894 ± 1.389 | 19.848 ± 2.210 | 24.801 ± 5.046 | 26.663 ± 4.103 | 34.983 ± 2.904 | 36.142 ± 1.712 |
| 200 Hz | 7.140 ± 1.188 | 8.056 ± 1.466 | 23.835 ± 5.215 | 27.734 ± 4.907 | 30.066 ± 4.307 | 47.416 ± 4.531 | 48.089 ± 3.533 |
| $F$ | 2.750 | 0.058 | 4.459 | 1.563 | 2.945 | 48.040 | 83.349 |
| $p$ | *0.115* | *0.813* | *0.049* | *0.227* | *0.103* | *0.000* | *0.000* |
| 200 Hz | 7.140 ± 1.188 | 8.056 ± 1.466 | 23.835 ± 5.215 | 27.734 ± 7.907 | 30.066 ± 4.307 | 47.416 ± 4.531 | 48.089 ± 3.533 |
| 500 Hz | 11.826 ± 2.218 | 11.706 ± 2.359 | 24.933 ± 4.344 | 34.890 ± 3.962 | 37.689 ± 6.786 | 51.313 ± 2.754 | 51.811 ± 2.107 |
| $F$ | 31.202 | 15.546 | 0.236 | 11.587 | 8.095 | 4.862 | 7.369 |
| $p$ | 0.000 | 0.000 | 0.633 | 0.003 | 0.011 | 0.041 | 0.014 |

*Note*: Results were considered statistically significant if $p < 0.05$, $n = 10$.

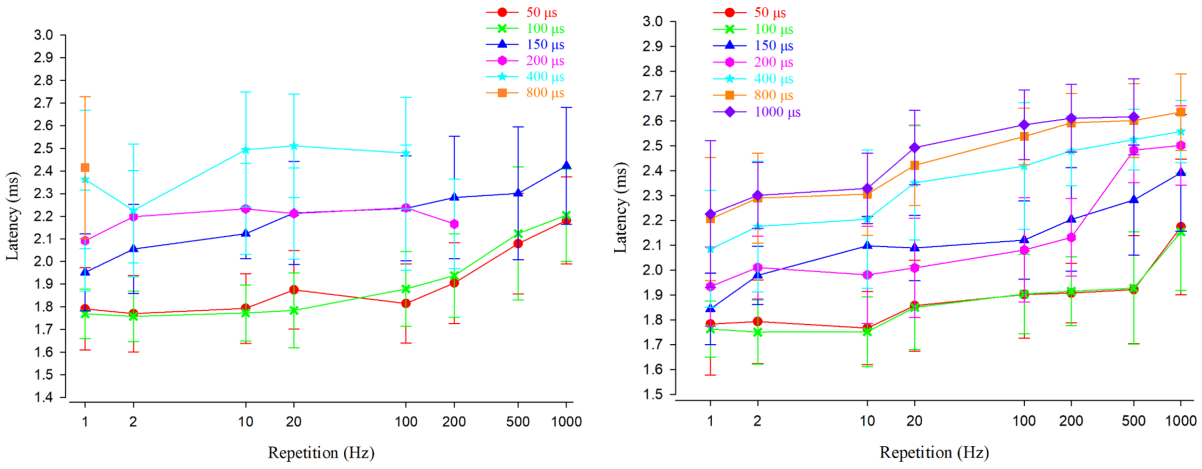


(a) (b)

Fig. 4. Latencies of oABRs at different pulse durations and repetition rates. (a) Latencies for an energy of 30 $\mu$J. (b) Latencies for an energy of 60 $\mu$J. Latencies are significantly higher ($p < 0.05$, $n = 10$) when the pulse duration increases from 100 $\mu$s to 150 $\mu$s, and from 200 $\mu$s to or over 400 $\mu$s. Latencies increase with increasing repetition rates while durations are fixed between 50 $\mu$s and 1000 $\mu$s. oABR, optical auditory brainstem response.

Table 3. Amplitudes between the pulse duration of 100 $\mu$s and 150 $\mu$s (Means $\pm$ SD, $n = 10$).

| | 1 Hz | 2 Hz | 10 Hz | 20 Hz | 100 Hz | 200 Hz | 500 Hz | 1000 Hz |
|---|---|---|---|---|---|---|---|---|
| 100 $\mu$s | 2.26 $\pm$ 0.271 | 2.20 $\pm$ 0.209 | 2.32 $\pm$ 0.084 | 2.29 $\pm$ 0.071 | 2.23 $\pm$ 0.026 | 2.17 $\pm$ 0.044 | 2.20 $\pm$ 0.036 | 2.17 $\pm$ 0.031 |
| 150 $\mu$s | 1.76 $\pm$ 1.842 | 1.83 $\pm$ 0.373 | 1.80 $\pm$ 0.076 | 1.68 $\pm$ 0.134 | 1.71 $\pm$ 0.108 | 1.76 $\pm$ 0.082 | 1.59 $\pm$ 0.110 | 1.17 $\pm$ 0.143 |
| $F$ | 12.903 | 7.245 | 17.004 | 18.487 | 19.681 | 13.168 | 26.674 | 58.620 |
| $p$ | *0.002* | *0.015* | *0.001* | *0.000* | *0.000* | *0.002* | *0.000* | *0.000* |

*Note*: Results were considered statistically significant if $p < 0.05$, $n = 10$.

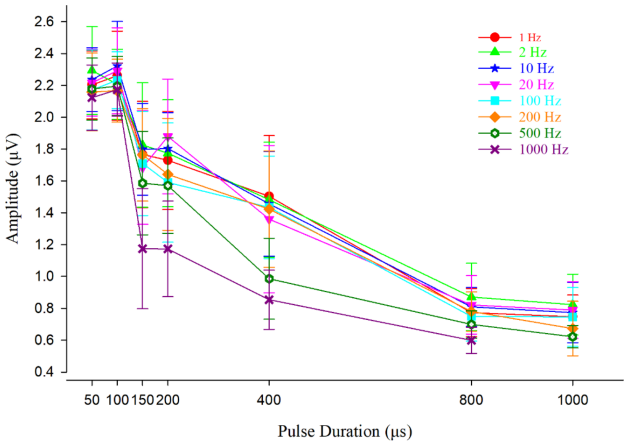


Fig. 5. Amplitudes of oABR wave III at different pulse durations and repetition rates. Data are shown as the mean $\pm$ SD ($n = 10$) and results are considered statistically significant if $p < 0.05$. The stimulus energy intensity was 60 $\mu$J. Amplitudes decrease significantly ($p < 0.05$, $n = 10$) when the pulse duration increases from 100 $\mu$s to 150 $\mu$s. There are no significant differences for pulse durations below 100 $\mu$s and above 800 $\mu$s regardless of the stimulus repletion rate. oABR, optical auditory brainstem response.

high stimulation frequency up to 19 kHz (or 9 kHz when a 100-$\mu$s duration was used). An identifiable oABR wave could be evoked by repetition rates even reaching 19 kHz while the energy increased. The energy threshold of oABRs was significantly elevated when the stimulus repetition rate increased from 200 Hz to 500 Hz (Table 2, Fig. 7; 200 Hz $7.140 \pm 1.188$, 500 Hz $11.826 \pm 2.218$; $F = 31.202$, $p < 0.001$), and from 5 kHz to 10 kHz (Table 7; 5 kHz $14.83 \pm 1.937$, 10 kHz $17.96 \pm 1.735$; $F = 12.995$, $p = 0.002$) at a 50-$\mu$s duration stimulation. When a 100-$\mu$s duration was used, the energy threshold was significantly elevated as the stimulus repetition rate increased from 200 Hz to 500 Hz (Table 2, Fig. 7), and then the oABR thresholds were elevated as the repetition rate increased without significant differences as the repetition rate climbed (Table 7, Fig. 7).

The temperature elevations varied in a pattern similar to that of the increases in energy thresholds. The temperature elevation significantly increased in

Table 4. Amplitudes between different stimulus repetitions (Means ± SD, $n = 10$).

| | 50 $\mu$s | 100 $\mu$s | 150 $\mu$s | 200 $\mu$s | 400 $\mu$s | 800 $\mu$s | 1000 $\mu$s |
|---|---|---|---|---|---|---|---|
| 200 Hz | 2.16 ± 0.059 | 2.17 ± 0.037 | 1.76 ± 0.084 | 1.64 ± 0.116 | 1.42 ± 0.133 | 0.78 ± 0.021 | 0.67 ± 0.036 |
| 500 Hz | 2.18 ± 0.043 | 2.20 ± 0.026 | 1.59 ± 0.108 | 1.57 ± 0.008 | 0.99 ± 0.058 | 0.70 ± 0.016 | 0.62 ± 0.009 |
| $F$ | 0.037 | 0.115 | 1.669 | 0.237 | 9.626 | 2.927 | 0.760 |
| $p$ | *0.849* | *0.438* | *0.213* | *0.632* | *0.006* | *0.104* | *0.395* |
| 500 Hz | 2.18 ± 0.04 | 2.20 ± 0.03 | 1.59 ± 0.11 | 1.57 ± 0.09 | 0.99 ± 0.06 | 0.70 ± 0.007 | * |
| 1000 Hz | 2.12 ± 0.04 | 2.17 ± 0.03 | 1.17 ± 0.14 | 1.17 ± 0.09 | 0.85 ± 0.03 | 0.60 ± 0.012 | |
| $F$ | 0.378 | 0.085 | 6.857 | 8.754 | 3.752 | 7.088 | |
| $p$ | *0.546* | *0.774* | *0.017* | *0.008* | *0.042* | *0.016* | |

*Note*: *When a pulse duration of 1000 $\mu$s was used, the stimulus repetition cannot be reached to 1000 Hz.
Results were considered statistically significant if $p < 0.05$, $n = 10$.

Table 5. Temperature variations between different pulse durations (Means ± SD, $n = 10$).

| | 1 Hz | 2 Hz | 10 Hz | 20 Hz | 100 Hz | 200 Hz | 500 Hz | 1000 Hz |
|---|---|---|---|---|---|---|---|---|
| 200 $\mu$s | 0.68 ± 0.011 | 0.72 ± 0.006 | 0.82 ± 0.017 | 1.01 ± 0.014 | 1.08 ± 0.022 | 1.15 ± 0.025 | 1.43 ± 0.027 | 2.67 ± 0.042 |
| 400 $\mu$s | 0.79 ± 0.019 | 0.76 ± 0.009 | 1.33 ± 0.018 | 1.35 ± 0.014 | 1.48 ± 0.026 | 1.53 ± 0.016 | 1.62 ± 0.037 | 3.09 ± 0.028 |
| $F$ | 4.109 | 1.029 | 73.845 | 40.961 | 33.333 | 35.508 | 5.631 | 25.200 |
| $p$ | *0.058* | *0.324* | *0.000* | *0.000* | *0.000* | *0.000* | *0.029* | *0.000* |

*Note*: Results were considered statistically significant if $p < 0.05$, $n = 10$.

both durations when increasing the stimulus repetition rate from 1 kHz to 2 kHz (Table 8, duration of 50 $\mu$s, 1 kHz 1.62 ± 0.209, 2 kHz 1.98 ± 0.223; $F =$ 12.515, $p = 0.002$; duration of 100 $\mu$s, 1 kHz 1.84 ± 0.201, 2 kHz 1.96 ± 0.215; $F = 29.896$, $p < 0.001$) and higher (Table 8, Fig. 8). There was no significant difference in temperature elevation for pulse durations of 50–100 $\mu$s when the stimulus repetition rate was 2 kHz and < 500 Hz (Table 8, Fig. 8).

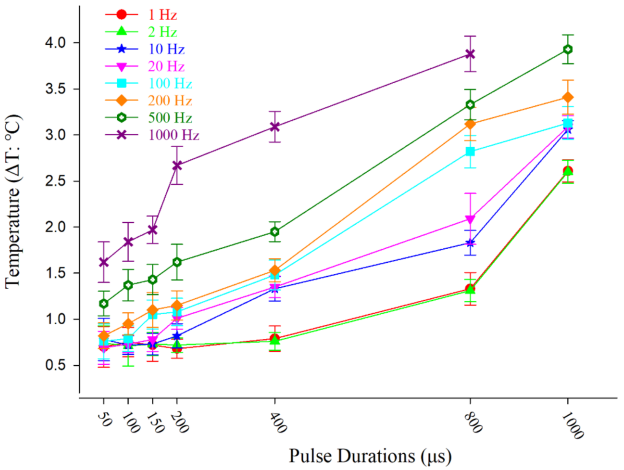


Fig. 6. Temperature variation curves on the site of stimulation at different pulse durations and repletion rates. The stimulus energy intensity was 60 $\mu$J. Data are shown as the mean ± SD ($n = 10$) and results are considered statistically significant if $p < 0.05$. There are no differences in temperature elevation when the repetition rate increases from 1 Hz to 2 Hz for any pulse duration.

### 3.6. *Hearing level changes pre- and post-INS*

We recorded aABRs in all animals prior to any other manipulation to confirm they had normal hearing and again at the end of the INS to evaluate the hearing changes post-stimulation. The threshold was elevated only at 32 kHz; however, the control ear also showed elevated thresholds for this frequency, while no significant differences in hearing loss were found between left and right ears (Fig. 9) in all 10 guinea pigs.

## 4. Discussion

INS has been proven as an alternative method to electrical stimulation because of its advantages in greater spatial resolution, higher accuracy, and no stimulation artifacts.[8–10] However, a safe and optimal stimulation model should be set up prior to

Table 6. Temperature variations between different stimulus repetitions (Means ± SD, $n = 10$).

| | 50 $\mu$s | 100 $\mu$s | 150 $\mu$s | 200 $\mu$s | 400 $\mu$s | 800 $\mu$s | 1000 $\mu$s |
|---|---|---|---|---|---|---|---|
| 2 Hz | 0.74 ± 0.036 | 0.71 ± 0.048 | 0.73 ± 0.016 | 0.72 ± 0.006 | 0.76 ± 0.009 | 1.31 ± 0.014 | 2.60 ± 0.016 |
| 10 Hz | 0.78 ± 0.053 | 0.72 ± 0.011 | 0.73 ± 0.013 | 0.82 ± 0.017 | 1.33 ± 0.018 | 1.83 ± 0.018 | 3.06 ± 0.009 |
| $F$ | 0.180 | 0.017 | 0.000 | 4.245 | 119.351 | 83.917 | 85.018 |
| $p$ | *0.676* | *0.897* | *1.000* | *0.054* | *0.000* | *0.000* | *0.000* |
| 20 Hz | 0.69 ± 0.032 | 0.73 ± 0.009 | 0.78 ± 0.017 | 1.01 ± 0.014 | 1.35 ± 0.014 | 2.09 ± 0.077 | 3.09 ± 0.014 |
| 100 Hz | 0.76 ± 0.036 | 0.79 ± 0.019 | 1.05 ± 0.025 | 1.08 ± 0.022 | 1.48 ± 0.026 | 2.82 ± 0.031 | 3.13 ± 0.031 |
| $F$ | 0.719 | 1.296 | 17.221 | 1.357 | 4.213 | 49.701 | 0.351 |
| $p$ | *0.407* | *0.270* | *0.001* | *0.259* | *0.055* | *0.000* | *0.561* |
| 200 Hz | 0.82 ± 0.020 | 0.95 ± 0.014 | 1.10 ± 0.036 | 1.15 ± 0.025 | 1.53 ± 0.016 | 3.12 ± 0.033 | 3.41 ± 0.034 |
| 500 Hz | 1.17 ± 0.018 | 1.37 ± 0.029 | 1.43 ± 0.027 | 1.62 ± 0.037 | 1.95 ± 0.012 | 3.33 ± 0.027 | 3.93 ± 0.025 |
| $F$ | 32.715 | 41.130 | 17.471 | 35.439 | 64.537 | 7.391 | 45.917 |
| $p$ | *0.000* | *0.000* | *0.001* | *0.000* | *0.000* | *0.014* | *0.000* |

*Note*: Results were considered statistically significant if $p < 0.05$, $n = 10$.

translating the technique into CI development. Laser parameters are important for establishing such a model. Although some previous studies have focused on laser parameters such as wavelength, pulse duration, stimulation repetitions, and stimulus energy,[21,25,26] most of them used low-frequency repetitions and short pulse durations. However, damage during INS is a purely thermal phenomenon, especially when using short pulse durations.[15] In this study, we designed an optrode to investigate the higher stimulus repetitions of INS and simultaneously record the local cumulative temperature variations during stimulation.

The energy thresholds of oABRs increased as the pulse duration became longer, reaching a plateau for pulse durations $\geq$200 $\mu$s, and the stimulus repetitions increased. Shorter pulse durations presented shorter latencies when constant stimulus repetition and energy were used in this study. The amplitudes of the oABRs significantly decreased when the pulse duration increased from 100 $\mu$s to $\geq$150 $\mu$s. These results demonstrate that shorter pulse durations require lower energy to evoke validated oABR waveforms and present larger

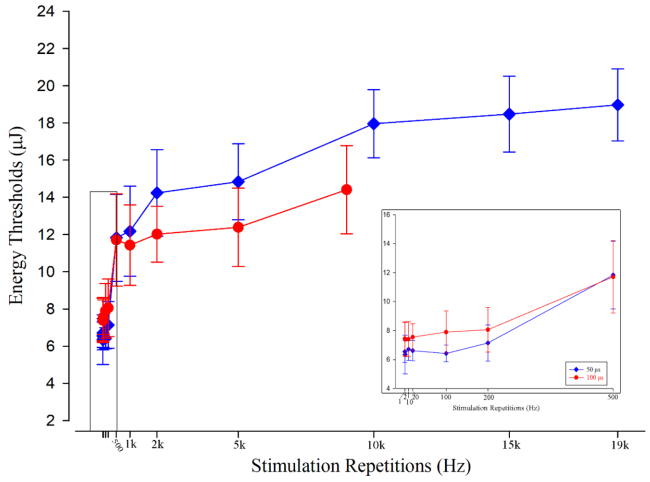


Fig. 7. oABR energy thresholds at different stimulation repetition rates. Data are shown as the mean ± SD ($n = 10$) and results are considered statistically significant if $p < 0.05$. The inset shows a magnification for repetition rates <500 Hz. Energy thresholds are not significantly different between pulse durations of 50 $\mu$s and 100 $\mu$s for repetition rates up to 500 Hz but become significantly different for repetition rates of 1 kHz and higher ($p < 0.05$, $n = 10$). oABR, optical auditory brainstem response.

Table 7. Thresholds of oABRs in high repetitions (Means ± SD, $n = 10$).

| | 50 $\mu$s | 100 $\mu$s | $F$ | $p$ |
|---|---|---|---|---|
| 1 kHz | 12.18 ± 2.295 | 11.426 ± 2.408 | 0.534 | 0.475 |
| 2 kHz | 14.24 ± 2.206 | 12.017 ± 1.419 | 6.448 | 0.021 |
| $F$ | 3.777 | 0.506 | | |
| $p$ | *0.068* | *0.486* | | |
| 2 kHz | 14.24 ± 2.206 | 12.017 ± 2.239 | | |
| 5 kHz | 14.83 ± 1.937 | 12.383 ± 4.435 | 6.982 | 0.017 |
| $F$ | 0.372 | 0.201 | | |
| $p$ | 0.549 | 0.659 | | |
| 5 kHz | 14.83 ± 1.937 | 12.383 ± 4.435 | | |
| 10 kHz (9 kHz)* | 17.96 ± 1.735 | 14.47 ± 2.247 | 14.089 | 0.001 |
| $F$ | 12.995 | 4.079 | | |
| $p$ | *0.002* | *0.059* | | |

*Note*: *When a pulse duration of 100 $\mu$s was used, the repetition cannot reach to 10 kHz.
Results were considered statistically significant if $p < 0.05$, $n = 10$.

Table 8. Temperature variations in high repetitions (Means ± SD, $n = 10$).

| | 50 $\mu$s | 100 $\mu$s | $F$ | $p$ |
|---|---|---|---|---|
| 1 kHz | 1.62 ± 0.209 | 1.84 ± 0.201 | 5.186 | 0.035 |
| 2 kHz | 1.98 ± 0.223 | 1.96 ± 0.215 | 0.038 | 0.849 |
| $F$ | 12.515 | 29.896 | | |
| $p$ | *0.002* | *0.000* | | |
| 2 kHz | 1.98 ± 0.223 | 1.96 ± 0.215 | | |
| 5 kHz | 6.32 ± 0.331 | 6.69 ± 0.281 | 6.536 | 0.020 |
| $F$ | 1064.827 | 1606.592 | | |
| $p$ | 0.000 | 0.000 | | |
| 5 kHz | 6.32 ± 0.331 | 6.69 ± 0.281 | | |
| 10 kHz (9 kHz)* | 6.92 ± 0.710 | 7.75 ± 0.454 | 8.731 | 0.008 |
| $F$ | 5.284 | 35.432 | | |
| $p$ | *0.034* | *0.000* | | |

*Note*: *When a pulse duration of 100 $\mu$s was used, the repetition cannot reach to 10 kHz.
Results were considered statistically significant if $p < 0.05$, $n = 10$.

amplitudes and shorter latencies. The pulse duration of 1000 $\mu$s could also evoke validated waveforms when enough energy was outputted. The energy threshold was 51.811 ± 2.107$\mu$J/pulse for 1000-$\mu$s pulses at 500 Hz repetition rate. Previous studies have demonstrated that structural damage by INS of the cochlea can be avoided under

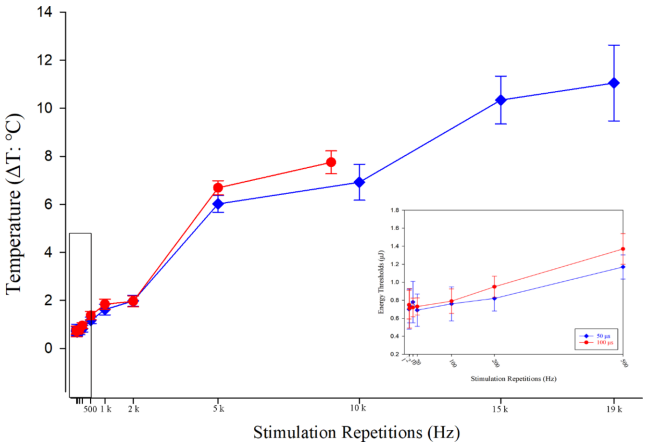


Fig. 8. Temperature variation on the site of stimulations for different repetition rates. Data are shown as the mean ± SD ($n = 10$) and results are considered statistically significant if $p < 0.05$. There is no significant difference in temperature elevation for pulse durations of 50–100 $\mu$s, when the stimulus repetition rate is 2 kHz (50 $\mu$s vs. 100 $\mu$s, $p = 0.849$, $n = 10$). The inset shows a magnification of the curve for repetition rates < 500 Hz. The temperature variation for pulse durations of 50–100 $\mu$s is not significantly different for repetition rates of up to 200 Hz.

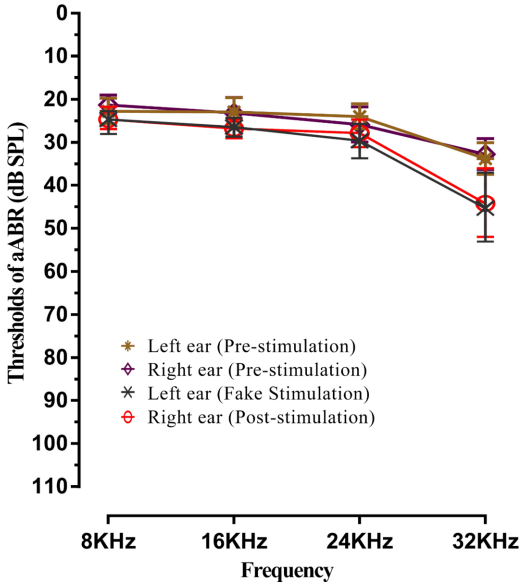


Fig. 9. aABR thresholds pre- and post-INS. Data are shown as the mean ± SD ($n = 10$) and results are considered statistically significant if $p < 0.05$. The brown and purple lines represent the aABR thresholds (dB SPL) of the left and right ears, respectively, before stimulation. The black line shows the threshold of aABRs in the left ear that underwent a fake stimulation postoperatively as the control group. The red line shows the aABR post-stimulation thresholds of the right ear. The results reveal no statistically significant differences. aABR, acoustically evoked auditory brainstem response; INS, infrared neural stimulation.

long-term exposure with energy below 100 $\mu$J/pulse and a repetition rate of 250 Hz.[27–29] Although longer pulse duration (with lower peak power) can be applied successfully to evoke validated waveforms, they require higher energy output to evoke an equivalent magnitude of wave amplitudes. Our results suggest that shorter pulse duration is a better choice for INS when using a wavelength of 1850 nm, as shorter pulses could be more energy efficient for INS. This was in accordance with the viewpoints of Izzo and colleagues[30] who suggested that longer pulse durations required higher radiant exposures to evoke the same magnitude compound action potential, because of the higher absorption coefficient of water in longer pulse durations. They suggested that more radiant energy was absorbed by the water around the radiation spot when a longer pulse duration was used; thus, the change of wavelength can have a significant impact on the light distribution in the tissue.[30] The peak power rather than the total energy of the pulse is the important factor for INS of the cochlea.[31] Moreover, shorter pulse durations

become even more important when aiming to minimize the effects of tissue heating during stimulation and prolong potential battery life.[32] Even though shorter pulses are considered to have a relatively lower margin of energy threshold for damage,[15] in theory, they allow relatively higher repetitions to be implemented during INS.

A previous study reported that pulse durations as short as 35 $\mu$s can evoke stable compound action potential responses at a repetition rate of 13 Hz.[21] However, the limitation of that study was the low stimulus repetition rate. Most publications report results obtained using low stimulation repetition rates.[8,24,25,28,29,33,34] Thus, there is a need to thoroughly investigate higher stimulation repetition rates, as they mimic the native firing patterns of the auditory nervous system and the electrical stimulation models used in CIs. In this study, we found that when the pulse duration was 50 $\mu$s, stable oABR waves were evoked even when stimulus repetition reached 19 kHz. The high repetition rate of stimulation was also effective in evoking oABRs when the energy was high and the pulse duration was short enough. When pulse duration was 50 or 100 $\mu$s, we found that the energy threshold increased as the stimulation repetition rate increased but reached a plateau when the repetition rate increased to 2 kHz (14.24 $\mu$J for 50-$\mu$s pulses, 12.02 $\mu$J for 100-$\mu$s pulses). As such, the energy threshold elevation curves increased nonlinearly. The phase-locking property of the SGNs ensures microsecond precision of sound encoding with high fidelity.[23] The temporal fine structure of a sound is the cycle-by-cycle timing of the waveform.[35] In theory, SGN phases locked to higher frequencies of stimulations should include spikes for acute responses for receiving a temporal perception of sound. In this case, a higher repetition rate of stimulation seems better than a lower rate for INS. In our study, higher stimulus repetitions needed higher energy to evoke validated oABR waveforms, especially when the pulse duration was longer than 200 $\mu$s. The oABR waveforms induced by the higher repetition rate have longer latencies and smaller amplitudes. These data indicate that higher repetition stimulus may contain some ineffective stimuli that fail to excite the SGNs, as longer latencies and smaller amplitudes were presented in higher repetition rates. Otherwise, the refractory period would limit the reaction of neurons to the INS; furthermore, INS may present inhibiting effects during radiation in certain parameters. Both the refractory period of neurons and the inhibiting effect of INS may affect INS efficiency. Duke and colleagues[36] combined infrared and electrical signals to stimulate buccal nerve 2 of *Aplysia* and rat sciatic nerve and found that high-frequency (200 Hz) infrared pulses ($\lambda = 1450$ nm, $\tau_{po} = 0.25$ ms) block propagation or inhibited the generation of action potentials evoked by electrical stimulation. Both low- and high-energy infrared (1450–1600 nm) irradiation itself can suppress or inhibit neuronal firing activity *in vivo*.[19] However, whether a similar blockage or inhibition effect occurred with INS in this study was not clear. Auditory nerve fibers phase-lock to higher frequencies when stimulated electrically than when stimulated with sound. However, even with pulse repetition rates $\geq$ 2 kHz, CI users show poorer sensitivity to temporal fine structure than do normal-hearing listeners.[35,37] Although our results demonstrated that a higher stimulation repetition rate ($\geq$ 2 kHz) evokes stable oABR waveforms, this requires higher energy and is accompanied by longer latency. This indicates that a higher INS repetition rate is not always better. However, whether this phenomenon was attributable to the phase-locking property of SGNs, the characteristics of different infrared parameters, or INS mechanisms should be illuminated in future studies. Otherwise, the relationship between stimulus repetitions and speech reception is more complicated, and the optimal and suitable repetition rates in INS need to be researched in more detail.

The likely mechanism of INS is an optothermal effect, by which optical stimulation locally and transiently increases the tissue temperature, as the optical energy is absorbed by water and converted into heat, leading to depolarization of the neurons.[8,38,39] The thermal response is essentially confined to the zone of optical irradiation, and the heat diffusion is negligible during the pulse; thus, the temperature increases linearly to a maximum value determined by the pulse energy and with a slope determined by peak power.[32] A change in temperature, rather than absolute temperature, is the key factor for initiating neuronal excitation in INS.[39,40] In this study, we monitored variations in the temperature of the liquid around the infrared radiation zone during stimulation. Our results showed that the temperature elevation was associated with both pulse duration and stimulus repetition rate. The temperature variations ramped up as the pulse

duration became longer and as the repetition rate increased. This may be because more radiant energy is absorbed and more temperature accumulation occurs before heat dissipates from the radiation zone when the pulse duration is longer and the repetition rate is higher. This is different from the results of several reports indicating that for a fixed pulse energy, longer pulse duration provides slower heating, evoking smaller neural responses than do shorter pulse durations.[30,38,41,42] However, the data of those reports were derived from mathematical calculations through formulae of thermal absorption coefficients of infrared pulses in water. Differences in the results could be accounted for by evaluating the different methods used to obtain the data. In this study, the temperature variations were monitored *in vivo* directly during the INS, rather than obtained from mathematical methods.

When a fixed pulse energy and repetition rate were used, temperature variations were significantly different while the pulse duration increased from 200 $\mu$s to 400 $\mu$s, except when the repetition rate was lower than 10 Hz. These results suggest that a pulse duration $\leq 200\mu$s results in lower temperature variations than do longer pulses. This finding is consistent with those of previous reports recommending pulse durations in the range of $\sim 20-200\,\mu$s for oCI development.[30,38,41,42] When we compared the temperature variations among different repetition rates using constant energy and pulse duration, we found that they increased as the repetition rate increased. Once the repetition rate increased from 200 Hz to 500 Hz, temperature variations varied significantly regardless of the pulse duration used. These results suggest that in higher repetition rate stimulations, heat probably accumulates adjacent to the radiation zones. Heat deposition in the tissue is the main disadvantage of INS, and this could be an obstacle for the development of implantable devices such as CIs.[43] Local temperature is increased by infrared radiation, with a thermal relaxation time of approximately 0.75–1.25 s, and a variable temperature in accordance with the fast pulse approximation.[44] When a high repetition rate of stimulation is used, thermal energy does not fully diffuse when the next pulse arrives, allowing thermal accumulation and local temperature to ramp up. In our study, the temperature variation trend was associated with the energy threshold elevation curves in a nonlinear fashion. The temperature increased dramatically when the repetition rate increased from 2 kHz to 5 kHz, and there were significant differences for both pulse durations used (50 $\mu$s and 100 $\mu$s).

The limitation inherent to directly recording the temperature elevation in this study is that our data reflect only the heat accumulating around the radiated site and not the real temperature changes of the tissue itself. Moreover, the response time of the probes was 200 ms in liquid, which is a few orders of magnitude longer than the actual infrared pulse durations. Moreover, the four probes, although being in contact with the tissue, were outside the area directly illuminated by the infrared emission. Thus, the temperature variations recorded in this study only reflected the accumulated temperature at 200 ms following the last pulse.

The thresholds of aABR were recorded to evaluate the hearing function pre- and post-INS. The left ear was subjected to the same surgical procedures, and an implanted fake optrode was used as a control. There were no significant differences in hearing levels between the stimulated and the control ear. The elevated thresholds of aABR at a frequency of 32 kHz were probably due to the lymphatic fistula induced by cochleotomy at the basilar turn. INS did not directly induce hearing loss in this study. Our results demonstrate that high repetition rates of INS cannot affect the hearing functions of animals.

In summary, INS at a high repetition rate can safely evoke stable and available oABRs in normal-hearing guinea pigs. However, INS elevated the temperature around the stimulus site area via a mechanism involving thermal accumulation during radiation, especially when a higher repetition stimulus was used. Shorter pulse durations ($\leq 200\,\mu$s) and repetition rates $\leq 2$ kHz are a better choice for INS when using a wavelength of 1850 nm, as these parameters could be more energy efficient without creating high gradients of temperature increases. Moreover, higher repetition stimulations induced longer latencies and smaller amplitudes of oABRs. Thus, higher repetition rates did not always improve results.

## 5. Ethics Policies

Animal care and use in this study were carried out in accordance with the National Health Commission of the People's Republic of China Guide for the Care and Use of Laboratory Animals and were

approved by the Animal Care and Use Committee of the Second Affiliated Hospital of Nanchang University.

## Conflict of Interest

Authors report no conflict of interest.

## Acknowledgments

Thanks Mr. Wan Qiwen for drawing the schematic diagram of the optrode. This work was supported by grants from the National Natural Science Foundation of China (81660173), the Natural Science Foundation of Jiangxi Province (20202BABL206065), and the Key Research and Development Program of Jiangxi Province (20181BBG78013).

## References

1. G. S. G. Geleoc, J. R. Holt, "Sound strategies for hearing restoration," *Science* **344**(6184), 1241062 (2014).
2. U. Müller, P. G. Barr-Gillespie, "New treatment options for hearing loss," *Nat. Rev. Drug Discov.* **14**(5), 346–365 (2015).
3. A. Dieter, C. J. Duque-Afonso, V. Rankovic, M. Jeschke, T. Moser, "Near physiological spectral selectivity of cochlear optogenetics," *Nat. Commun.* **10**(1), 1910–1962 (2019).
4. L. M. Friesen, R. V. Shannon, D. Baskent, X. Wang, "Speech recognition in noise as a function of the number of spectral channels: Comparison of acoustic hearing and cochlear implants," *J. Acoust. Soc. Am.* **110**(2), 1150–1163 (2001).
5. T. Dombrowski, V. Rankovic, T. Moser, "Toward the optical cochlear implant," *Cold Spring Harb. Perspect. Med.* **9**(8), a33225 (2018).
6. C. P. Richter, A. I. Matic, J. D. Wells, E. D. Jansen, J. T. Walsh, "Neural stimulation with optical radiation," *Laser Photonics Rev.* **5**(1), 68–80 (2011).
7. A. C. Thompson, P. R. Stoddart, E. D. Jansen, "Optical stimulation of neurons," *Curr. Mol. Imaging* **3**(2), 162–177 (2014).
8. B. Xie, C. Dai, H. Li, "Attenuated infrared neuron stimulation response in cochlea of deaf animals may associate with the degeneration of spiral ganglion neurons," *Biomed. Opt. Express* **6**(6), 1990–2005 (2015).
9. X. Tan, I. Jahan, Y. Xu, S. Stock, C. C. Kwan, C. Soriano, X. Xiao, J. García-Añoveros, B. Fritzsch, C.-P. Richter, "Auditory neural activity in congenitally deaf mice induced by infrared neural stimulation," *Sci. Rep.* **8**(1), 388 (2018).
10. L. Paris, I. Marc, B. Charlot, M. Dumas, J. Valmier, F. Bardin, "Millisecond infrared laser pulses depolarize and elicit action potentials on in-vitro dorsal root ganglion neurons," *Biomed. Opt. Express* **8** (10), 4568 (2017).
11. C.-P. Richter, X. Tan, "Photons and neurons," *Hear. Res.* **311**, 72–88 (2014).
12. H. Zhao, "Recent progress of development of optogenetic implantable neural probes," *Int. J. Mol. Sci.* **18**(8), 1751 (2017).
13. J. G. Bernstein, P. A. Garrity, E. S. Boyden, "Optogenetics and thermogenetics: Technologies for controlling the activity of targeted cells within intact neural circuits," *Curr. Opin. Neurobiol.* **22**(1), 61–71 (2012).
14. D. Nelidova, R. K. Morikawa, C. S. Cowan, Z. Raics, D. Goldblum, H. P. N. Scholl, T. Szikra, A. Szabo, D. Hillier, B. Roska, "Restoring light sensitivity using tunable near-infrared sensors," *Science* **368**(6495), 1108–1113 (2020).
15. W. L. Hart, T. Kameneva, A. K. Wise, P. R. Stoddart, "Biological considerations of optical interfaces for neuromodulation," *Adv. Opt. Mater.* **7**(19), 1900385 (2019).
16. V. Lumbreras, E. Bas, C. Gupta, S. M. Rajguru, "Pulsed infrared radiation excites cultured neonatal spiral and vestibular ganglion neurons by modulating mitochondrial calcium cycling," *J. Neurophysiol.* **112**(6), 1246–1255 (2014).
17. V. H. Hernandez, A. Gehrt, K. Reuter, Z. Jing, M. Jeschke, A. M. Schulz, G. Hoch, M. Bartels, G. Vogt, C. W. Garnham, H. Yawo, Y. Fukazawa, G. J. Augustine, E. Bamberg, S. Kügler, T. Salditt, L. de Hoz, N. Strenzke, T. Moser, "Optogenetic stimulation of the auditory pathway," *J. Clin. Invest.* **124**(3), 1114–1129 (2014).
18. C. Wrobel, A. Dieter, A. Huet, D. Keppeler, C. J. Duque-Afonso, C. Vogl, G. Hoch, M. Jeschke, T. Moser, "Optogenetic stimulation of cochlear neurons activates the auditory pathway and restores auditory-driven behavior in deaf adult gerbils," *Sci. Transl. Med.* **10**(449), eaao0540 (2018).
19. Á. C. Horváth, S. Borbély, Ö. C. Boros, L. Komáromi, P. Koppa, P. Barthó, Z. Fekete, "Infrared neural stimulation and inhibition using an implantable silicon photonic microdevice," *Microsyst. Nanoeng.* **6**(1), 44 (2020).
20. C. P. Richter, S. M. Rajguru, A. I. Matic, E. L. Moreno, A. J. Fishman, A. M. Robinson, E. Suh, J. T. Walsh, "Spread of cochlear excitation during

stimulation with pulsed infrared radiation: Inferior colliculus measurements," *J. Neural Eng.* **8**(5), 56006 (2011).
21. A. D. Izzo, J. T. Walsh, E. D. Jansen, M. Bendett, J. Webb, H. Ralph, C.-P. Richter, "Optical parameter variability in laser nerve stimulation: A study of pulse duration, repetition rate, and wavelength," *IEEE Trans. Biomed. Eng.* **54**(6), 1108–1114 (2007).
22. A. I. Matic, A. M. Robinson, H. K. Young, B. Badofsky, S. M. Rajguru, S. Stock, C. P. Richter, "Behaviored and electrophysiological responses evoked by chronic infrared neural stimulation of the cochlea," *PLOS One* **8**(3), e58189 (2013).
23. M. A. Rutherford, N. M. Chapochnikov, T. Moser, "Spike encoding of neurotransmitter release timing by spiral ganglion neurons of the cochlea," *J. Neurosci.* **32**(14), 4773–4789 (2012).
24. W. G. A. Brown, K. Needham, J. M. Begeng, A. C. Thompson, B. A. Nayagam, T. Kameneva, P. R. Stoddart, "Thermal damage threshold of neurons during infrared stimulation," *Biomed. Opt. Express* **11**(4), 2224 (2020).
25. M. Schultz, P. Baumhoff, H. Maier, I. U. Teudt, A. Kruger, T. Lenarz, A. Kral, "Nanosecond laser pulse stimulation of the inner ear — A wavelength study," *Biomed. Opt. Express* **3**(12), 3332–3345 (2012).
26. J. Wang, J. Lu, C. Li, L. Xu, X. Li, L. Tian, "Pulsed 980 nm short wavelength infrared neural stimulation in cochlea and laser parameter effects on auditory response characteristics," *Biomed. Eng. Online* **14**(1), 89 (2015).
27. P. Baumhoff, N. Kallweit, A. Kral, "Intracochlear near infrared stimulation: Feasibility of optoacoustic stimulation in vivo," *Hear. Res.* **371**, 40–52 (2019).
28. R. T. Richardson, A. C. Thompson, A. K. Wise, K. Needham, "Challenges for the application of optical stimulation in the cochlea for the study and treatment of hearing loss," *Expert Opin. Biol. Ther.* **17**(2), 213–223 (2017).
29. V. Goyal, S. Rajguru, A. I. Matic, S. R. Stock, C.-P. Richter, "Acute damage threshold for infrared neural stimulation of the cochlea: Functional and histological evaluation," *Anat. Rec.* **295**(11), 1987–1999 (2012).
30. A. D. Izzo, J. T. Walsh, Jr., H. Ralph, J. Webb, M. Bendett, J. Wells, C. P. Richter, "Laser stimulation of auditory neurons: Effect of shorter pulse duration and penetration depth," *Biophys. J.* **94**(8), 3159–3166 (2008).
31. R. M. Banakis, A. I. Matic, S. M. Rajguru, C.-P. Richter, "Optical stimulation of the auditory nerve: Effects of pulse shape," *Proc. SPIE* **7883**(1), 788358 (2011).
32. B. J. Norton, M. A. Bowler, J. D. Wells, M. D. Keller, "Analytical approaches for determining heat distributions and thermal criteria for infrared neural stimulation," *J. Biomed. Opt.* **18**(9), 98001 (2013).
33. X. Tan, S. Rajguru, H. Young, N. Xia, S. R. Stock, X. Xiao, C. P. Richter, "Radiant energy required for infrared neural stimulation," *Sci. Rep.* **5**, 13273 (2015).
34. A. C. Thompson, J. B. Fallon, A. K. Wise, S. A. Wade, R. K. Shepherd, P. R. Stoddart, "Infrared neural stimulation fails to evoke neural activity in the deaf guinea pig cochlea," *Hear. Res.* **324**, 46–53 (2015).
35. J. C. Middlebrooks, R. L. Snyder, "Selective electrical stimulation of the auditory nerve activates a pathway specialized for high temporal acuity," *J. Neurosci.* **30**(5), 1937–1946 (2010).
36. A. R. Duke, H. Lu, M. W. Jenkins, H. J. Chiel, E. D. Jansen, "Spatial and temporal variability in response to hybrid electro-optical stimulation," *J. Neural Eng.* **9**(3), 36003 (2012).
37. J. C. Middlebrooks, "Cochlear-implant high pulse rate and narrow electrode configuration impair transmission of temporal information to the auditory cortex," *J. Neurophysiol.* **100**(1), 92–107 (2008).
38. C.-P. Richter, R. Bayon, A. D. Izzo, M. Otting, E. Suh, S. Goyal, J. Hotaling, J. T. Walsh, "Optical stimulation of auditory neurons: Effects of acute and chronic deafening," *Hear. Res.* **242**(1–2), 42–51 (2008).
39. J. Wells, C. Kao, P. Konrad, T. Milner, J. Kim, A. Mahadevan-Jansen, E. D. Jansen, "Biophysical mechanisms of transient optical stimulation of peripheral nerve," *Biophys. J.* **93**(7), 2567–2580 (2007).
40. S. M. Rajguru, C. P. Richter, A. I. Matic, G. R. Holstein, S. M. Highstein, G. M. Dittami, R. D. Rabbitt, "Infrared photostimulation of the crista ampullaris," *J. Physiol.* **589**(Pt 6), 1283–1294 (2011).
41. S. M. Rajguru, A. I. Matic, A. M. Robinson, A. J. Fishman, L. E. Moreno, A. Bradley, I. Vujanovic, J. Breen, J. D. Wells, M. Bendett, C.-P. Richter, "Optical cochlear implants: Evaluation of surgical approach and laser parameters in cats," *Hear. Res.* **269**(1–2), 102–111 (2010).
42. M. J. Alemzadeh-Ansari, M. A. Ansari, M. Zakeri, M. Haghjoo, "Influence of radiant exposure and repetition rate in infrared neural stimulation with near-infrared lasers," *Lasers Med. Sci.* **34**(8), 1555–1566 (2019).

43. S.-R. Tsai, M. R. Hamblin, "Biological effects and medical applications of infrared radiation," *J. Photochem. Photobiol. B, Biol.* **170**, 197–207 (2017).
44. A. R. Duke, M. W. Jenkins, H. Lu, J. M. McManus, H. J. Chiel, E. D. Jansen, "Transient and selective suppression of neural activity with infrared light," *Sci. Rep.* **3**, 2600 (2013).